Determination of the Sea Surface Slope Distribution and Wind Velocity using Sun Glitter Viewed from a Synchronous Satellite[1]

NADAV LEVANON

Dept. of Environmental Sciences, Tel-Aviv University, Ramat-Aviv, Israel

(Manuscript received 15 March 1971, in revised form 8 April 1971)

ABSTRACT

This work demonstrates the feasibility of determining the east-west component of the sea surface slope distribution from a synchronous satellite, through quantitative analysis of the sun glitter.

The Cox-Munk sun glitter technique, utilizing a single photograph of the whole-sun glitter pattern, taken from an aircraft altitude, is adapted to a much higher altitude. This is done by making a sequence of light intensity measurements, reflected from a single point on the ocean, as this fixed point scans the westward moving sun glitter pattern.

Wind velocity is calculated from the slope variance, using the Cox-Munk empirical relation. Calculated wind velocities for three locations in the Pacific, on two separate days, are compared to direct wind measurements taken at these locations during the Line Islands Experiment. The agreement is within ± 1 m sec^{-1}.

1. Introduction

The use of sun glitter to study the slope statistics of the sea was suggested and explored by Cox and Munk (1954a,b). Their basic idea can be summarized as follows. If the sea surface were entirely calm, then an overhead observer would see a single, mirror-like reflection of the sun at the horizontal specular point. The sea, of course, is never mirror flat, but due to the short wavelength of light, it can be considered as being constructed from many small facets, each with its own inclination. The farther a facet is from the horizontal specular point, the greater is the inclination required to reflect light toward the observer. The location of the reflected light source can therefore be interpreted as a certain sea slope, and the average intensity of the light coming from this location can be interpreted as the frequency with which this particular slope occurs.

Cox and Munk estimated sea-slope distributions using sun glitter photographs taken from an aircraft. They also suggested an empirical relation between the variance of the slopes and the surface wind velocity.

With the advent of the ATS-1 synchronous satellite, sun glitter has appeared as a major phenomenon on the photographs received daily from the spin-scan camera.

The purpose of the present work is to adapt the Cox-Munk technique to pictures taken from a much larger altitude, by a synchronous satellite. The main modification involves the use of a sequence of photographs of a limited area (taken over a time period) rather than a single photograph of the whole sun glitter area.

Such data from the satellite were used to calculate the slope distribution, and from it the wind velocity, for the locations of Palmyra, Fanning and Christmas Islands, on 16 and 19 April 1967. The calculated values were compared to direct wind measurements obtained at these locations during the Line Islands Experiment (Zipser and Taylor, 1968).

Utilizing data from the scanning type electronic camera, it was possible to by-pass the highly degrading photographic and photometric processes and to do all the quantitative work on the received video signal.

2. The synchronous satellite as the observer

In their work, Cox and Munk photographed the sun glitter from aircraft altitudes, and studied the slope distribution from a single photograph. This was done by identifying each location within the glitter with the specific sea slope which would cause reflection at that location.

The basic assumption involved in using different locations within a single glitter is that the statistical characteristics of the sea surface are essentially constant over the whole area of the sun glitter. When the photograph is taken from an aircraft this assumption is true. However, when the photograph is taken from synchronous altitude (35,783 km), the sun glitter covers a circle whose diameter can exceed 3000 km; with such a large area the basic assumption is no longer plausible.

This point is brought out in Fig. 1, which shows a sequence of six photographs of the same portion of the ocean (5–15N, 160–230W), taken at intervals of $\sim$23 min. The sun glitter is apparent in all the frames, and its shift to the west can be clearly seen. Note the calm area of the ocean which appears as a dark area in the midst of the sun glitter in the second frame. In the third frame this area already includes the horizontal specular

[1] This paper was written while the author was at the Space Science and Engineering Center, University of Wisconsin, Madison.

point of reflection, and the light intensity reflected from part of it is greater than the light scattered from the clouds. In the last frame the specular point of reflection has moved outside the calm area and the sun glitter ends sharply at its edge. Thus, Fig. 1 shows that the sea roughness may vary considerably over a large glitter area. But we also note that the shape of the calm area did not change appreciably in the 2-hr period between the first and the last frame. This leads to an alternative assumption, *viz.*, that the statistical characteristics of the sea surface at a fixed point do not vary appreciably over a period of several hours.

Recalling that the synchronous satellite is in a fixed position relative to the earth while the horizontal specular point of reflection shifts with time from east to west, we see that this assumption allows us to adapt the Cox-Munk technique to the case of observation from a synchronous satellite. Specifically, the values of light intensity reflected toward the satellite from a fixed point at different times can be interpreted in terms of the sea slope distribution near that point.

3. The satellite, the points of reflection and the sun subpoint

The ATS-1 satellite is positioned over the equator at about 150W longitude. From a height of 35,783 km, its spin scan camera usually observes the portion of the earth bounded by 70W and 230W, and by 52.5N and 52.5S. This area is scanned by 2018 horizontal (west to east) lines. The optical resolution is 2.0 n mi when the telescope is pointed straight down. The normal down scan takes 20 min and the retrace an additional 2 min. The optical system bandpass is 4750–6300 Å. The camera video output is linear within $\pm 2\%$, up to the intensity of 10,000 foot lamberts.

The data at the ground station were available in three forms: as pictures, on analog tape, and on digital tape. On the digital tape, the maximum intensity was divided into 250 units, and each line into 8192 picture elements, of which the limb distance of an equatorial line occupies 7128 picture elements.

Special techniques were derived for navigation within the pictures. This utilized the simple method of two landmarks, Baja California and Hawaii, which were not overcast on the specific days used for analysis. The error involved with this method was less than 50 mi.

The points of reflection in our study corresponded to Palmyra Island (5°53′N 162°05′W), Fanning Island (3°54′N 159°23′W) and Christmas Island (1°55′N 157°20′W). Actual wind measurements were obtained on these three islands during the Line Islands Experiment.

On 16 April 1967, the sun subpoint traveled approximately along 10N, and on 19 April along 11N. The exact longitudes and latitudes of the sun subpoint as functions of time were obtained from the Air Almanac.

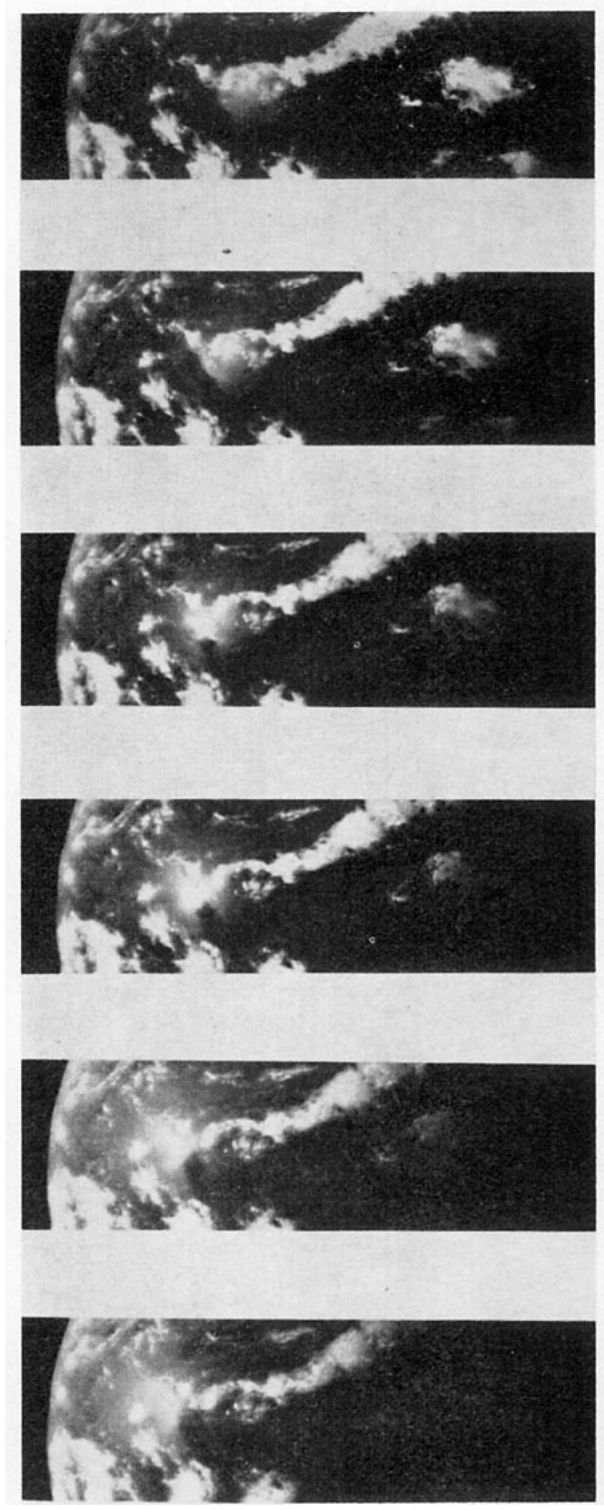

FIG. 1. Westward shift of the sun glitter over a calm area in the midst of a rough ocean. Pictures (from top to bottom) were taken at 0114:51, 0138:05, 0201:21, 0224:34, 0247:52 and 0311:05 GMT on 17 April 1967.

4. The geometry of reflection

In order to apply the method, we need an answer to the following geometrical question: given the longitude

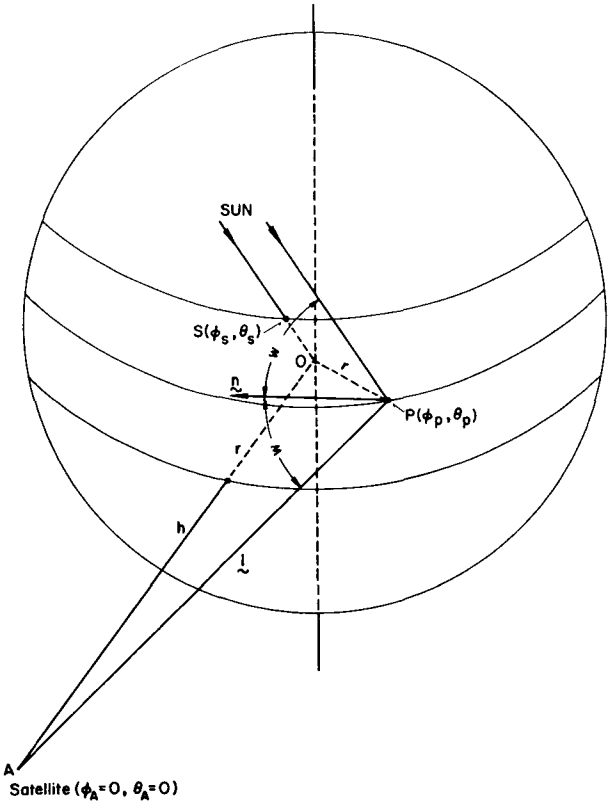

FIG. 2. The geometry of reflection.

and latitude of the sun and the synchronous satellite subpoints, and of the point of reflection, what is the tilt magnitude and direction and the angle of incidence, at that point of reflection?

To derive the necessary formulas we shall use the following notation (Fig. 2):

- O the center of the earth
- S the sun subpoint
- A the synchronous satellite
- P the point of reflection
- i an index taking values S, P, $\mathbf{l}$ or $\mathbf{n}$
- Q_i a point defined by the sea surface and a vector parallel to i and starting at O
- θ_i latitude of i (or of Q_i)
- ϕ_i longitude of A minus longitude of i (or of Q_i)
- r the radius of the earth
- h the synchronous altitude
- $\mathbf{l}$ vector between the satellite and the point of reflection
- $\mathbf{n}$ the normal required for reflection from P
- θ the northward tilt at P
- ϕ the eastward tilt at P
- β the magnitude of the total tilt at P
- ω the angle of incidence

An elementary manipulation of rectangular and spherical coordinates yields

$$\phi_l=\tan^{-1}\left[\frac{-r\cos\theta_p\sin\phi_p}{h+r(1-\cos\theta_p\cos\phi_p)}\right], \tag{1}$$

$$\theta_l=\tan^{-1}\left\{\frac{-r\sin\theta_p}{[(h+r)^2-2r(h+r)\cos\theta_p\cos\phi_p+r^2\cos^2\theta_p]^{\frac{1}{2}}}\right\}, \tag{2}$$

$$\phi_n=\tan^{-1}\left[\frac{\cos\theta_l\sin\phi_l+\cos\theta_s\sin\phi_s}{\cos\theta_l\cos\phi_l+\cos\theta_s\cos\phi_s}\right], \tag{3}$$

$$\theta_n=\tan^{-1}\left\{\frac{\sin\theta_l+\sin\theta_s}{[\cos^2\theta_l+\cos^2\theta_s+2\cos\theta_l\cos\theta_s\cos(\phi_l-\phi_s)]^{\frac{1}{2}}}\right\}. \tag{4}$$

At the point of reflection the tilt in the east (or ϕ) direction is given by

$$\phi=\phi_n-\phi_p, \tag{5}$$

and the tilt in the north (or θ) direction by

$$\theta=\theta_n-\theta_p. \tag{6}$$

Recalling that ϕ and θ are orthogonal, we get for the total tilt magnitude

$$\beta=\tan^{-1}[\tan^2\theta+\tan^2\phi]^{\frac{1}{2}}, \tag{7}$$

and for the angle of incidence

$$\omega=\tan^{-1}[\tan^2(\theta_n-\theta_s)+\tan^2(\phi_n-\phi_s)]^{\frac{1}{2}}. \tag{8}$$

If both the point of reflection and the sun subpoint are near the satellite subpoint, i.e., if all θ and ϕ values are small, the above equations can be approximated by the simplified formulas:

$$\phi\approx\frac{\phi_s}{2}-\left(1+\frac{r}{2h}\right)\phi_p, \tag{9}$$

$$\theta\approx\frac{\theta_s}{2}-\left(1+\frac{r}{2h}\right)\theta_p, \tag{10}$$

$$\beta^2 \approx \theta^2 + \phi^2, \tag{11}$$

$$\omega^2 \approx \frac{1}{4}\left(\theta_s + \frac{r}{h}\theta_p\right)^2 + \frac{1}{4}\left(\phi_s + \frac{r}{h}\phi_p\right)^2. \tag{12}$$

5. Slope probability and light intensity

Cox and Munk and Cox (1965)[2] have shown that the probability density P of the slope (determined by the location) is related to the received intensity J, from this location, according to:

$$P = [4H^{-1}\rho^{-1}(\omega)A^{-1}\cos\mu]J\cos^4\beta, \tag{13}$$

where H is the solar energy flux per unit area of beam, ω the angle of incidence, $\rho(\omega)$ the reflection coefficient, β the slope magnitude, A the telescope effective area, and μ the telescope tilt from nadir. They have calculated $\rho(\omega)$ for sea water to be 0.020, 0.021, 0.060 and 1.00 for $\omega = 0°$, 30°, 60° and 90°, respectively.

In our system (fixed satellite and single point of reflection), the angle μ is constant. Since ω is less than 30° for the case of small angles, $\rho(\omega)$ is also essentially constant. Therefore, the term in brackets in (15) does not vary with time, and the only variable correction is $\cos^4\beta$.

6. Background light

In addition to the sun glitter, other sources of radiation have to be considered. Cox and Munk pointed out two of them: 1) the skylight reflected at the sea surface, and 2) the sunlight scattered by particles beneath the sea surface. Rozenberg and Mullamaa (1965) pointed out another source: 3) the scattered light in the air column separating the satellite from the water surface. Undoubtedly there are more contributors to the background light.

Cox and Munk found that sources 1) and 2) depend mainly on the angle between the vertical and the vector from the point under analysis to the observer. In the case of an observer on a synchronous satellite this angle is fixed.

An indication of the third source, 3), i.e., the scattered light in the atmosphere, can be obtained from the maps of Sekera and Viezee (1961) even though they assume the satellite at infinity. We will use the maps calculated for the case of a planetary surface that absorbs all the incident radiation ($A = 0$), i.e., when the only return is from scattering in the atmosphere. Those maps indicate only slight variations in the intensity of the scattered light in the vicinity of the satellite subpoint, as the sun subpoint shifts away, as long as the angular distance between the sun and the satellite is smaller than ~40°. For our small angles case, we can therefore assume this contribution to be constant.

[2] Cox, C., 1965: The relation of backscattered radiation to wind-stress at the sea surface. Paper presented at the AGU-AMS Intern. Symp. on Electromagnetic Sensing of the Earth from Satellites, Miami, Fla.

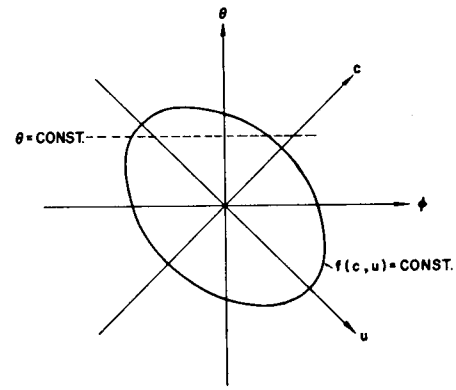

FIG. 3. The probability space of the two-dimensional normal distribution of the waves slope:

c slope in the crosswind direction
u slope in the upwind direction
ϕ slope in the east direction
θ slope in the north direction.

The above indicates that the background light can be estimated by measuring the radiation received from the point when it is outside the sun glitter limits.

The camera on the ATS-3 satellite has three channels: blue (0.38–0.48μ), green (0.48–0.58) and red (0.55–0.63), the respective background intensities being related to each other as 5:6:2, when calibrated for equal reflection from cloud tops. Thus, for reducing the background light, the red channel data is the best choice.

There is, of course, no way to study the sun glitter in the case of an overcast. However, in the case of scattered clouds, the present method (since it is based on measurements at a single point) can be used to study the wind velocity in any neighborhood within which a clear area of the size of the telescope resolution can be found.

7. The slope distribution

Cox and Munk found that the slope distribution is almost like a two-dimensional Gaussian (normal) distribution. To simplify our discussion we will assume the slope distribution to be Gaussian with zero mean. Thus, if c is the slope toward the crosswind direction and u toward the upwind direction, their probability density is given by

$$f(c,u) = \frac{1}{2\pi\sigma_c\sigma_u(1-r^2)^{\frac{1}{2}}} \times \exp\left[-\frac{1}{2(1-r^2)}\left(\frac{c^2}{\sigma_c^2} - \frac{2rcu}{\sigma_c\sigma_u} + \frac{u^2}{\sigma_u^2}\right)\right], \tag{14}$$

where σ_c and σ_u are the standard deviations of c and u, and r is their correlation coefficient.

Cox and Munk found that r is close to zero, i.e., c and u are approximately independent. In this case the c and u axes are the principal axes of the ellipses of constant density (Fig. 3). However, they will not, in

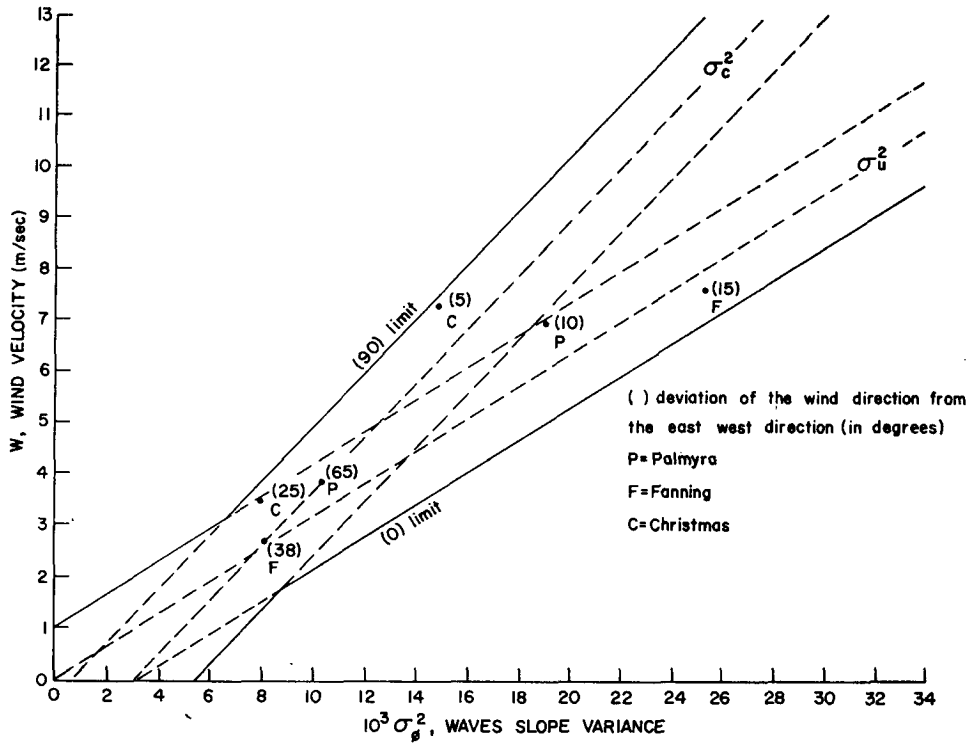

FIG. 4. The linear relation between the waves slope variance and the wind velocity (after Cox and Munk), compared to six points represented by variance calculated from the satellite data, and actual wind measurements.

general, coincide with the north (θ) and east (ϕ) axes, i.e., θ and ϕ will be jointly normal but correlated.

The sun glitter scan over a fixed point in the ocean may be considered equivalent to traversing the slope-probability plane along a certain path. Note that in (9) and (10) the only variable (with time) is the longitude of the sun subpoint ϕ_s. For the small angle case, we see that only ϕ varies with time while θ remains constant. Our path in the slope-probability plane is therefore a line θ = constant and the density P measured using (13) is (up to within a constant) the conditional probability density

$$f(\phi|\theta)=\text{constant}\times P. \tag{15}$$

This density is also normal, with the mean

$$E(\phi|\theta)=\frac{r\sigma_\phi}{\sigma_\theta}\theta, \tag{16}$$

and the standard deviation

$$\sigma_{\phi|\theta}=\sigma_\phi(1-r^2)^{\frac{1}{2}}, \tag{17}$$

where r is the correlation coefficient of ϕ and θ.

Cox and Munk found linear relations between the wind velocity W and the variances as

$$\sigma_c^2=0.003+1.92\times10^{-3}W\pm0.002, \tag{18}$$

$$\sigma_u^2=0.000+3.16\times10^{-3}W\pm0.004, \tag{19}$$

$$\sigma_c^2+\sigma_u^2=0.003+5.12\times10^{-3}W\pm0.004, \tag{20}$$

where σ is in radians and W is the mean wind in meters per seconds (measured 41 ft above the sea surface).

It can be shown (ignoring the anomaly of $\sigma_c\neq\sigma_u$ at no wind) that

$$|r|<\frac{\sigma_u^2-\sigma_c^2}{2\sigma_c^2}. \tag{21}$$

Using (18), (19) and (21) we find that $r<0.2$ up to average winds of 10 m sec^{-1}; this was the case 99.67% of the time, on the three islands during March and April. This and the small θ rules out any chance to use (16) as a clue for the wind direction. It also means that (17) will reduce to

$$\sigma_{\phi|\theta}\approx\sigma_\phi. \tag{22}$$

Eq. (22) indicates, as could be seen intuitively at the beginning of this section, that our method estimates the distribution of slopes in the east-west direction. We do not usually know whether this direction coincides with the upwind or cross wind direction, or with any other direction between the two. We, therefore, cannot use only one of Cox and Munk's linear relations between the wind velocity and the variance [Eqs. (18), (19)], but we must use the two of them together. This is done in Fig. 4 where the lines represent the two linear relations and their uncertainty boundaries. The lack of knowledge about the wind direction expands the range of possible wind velocities for each value of the slopes variance.

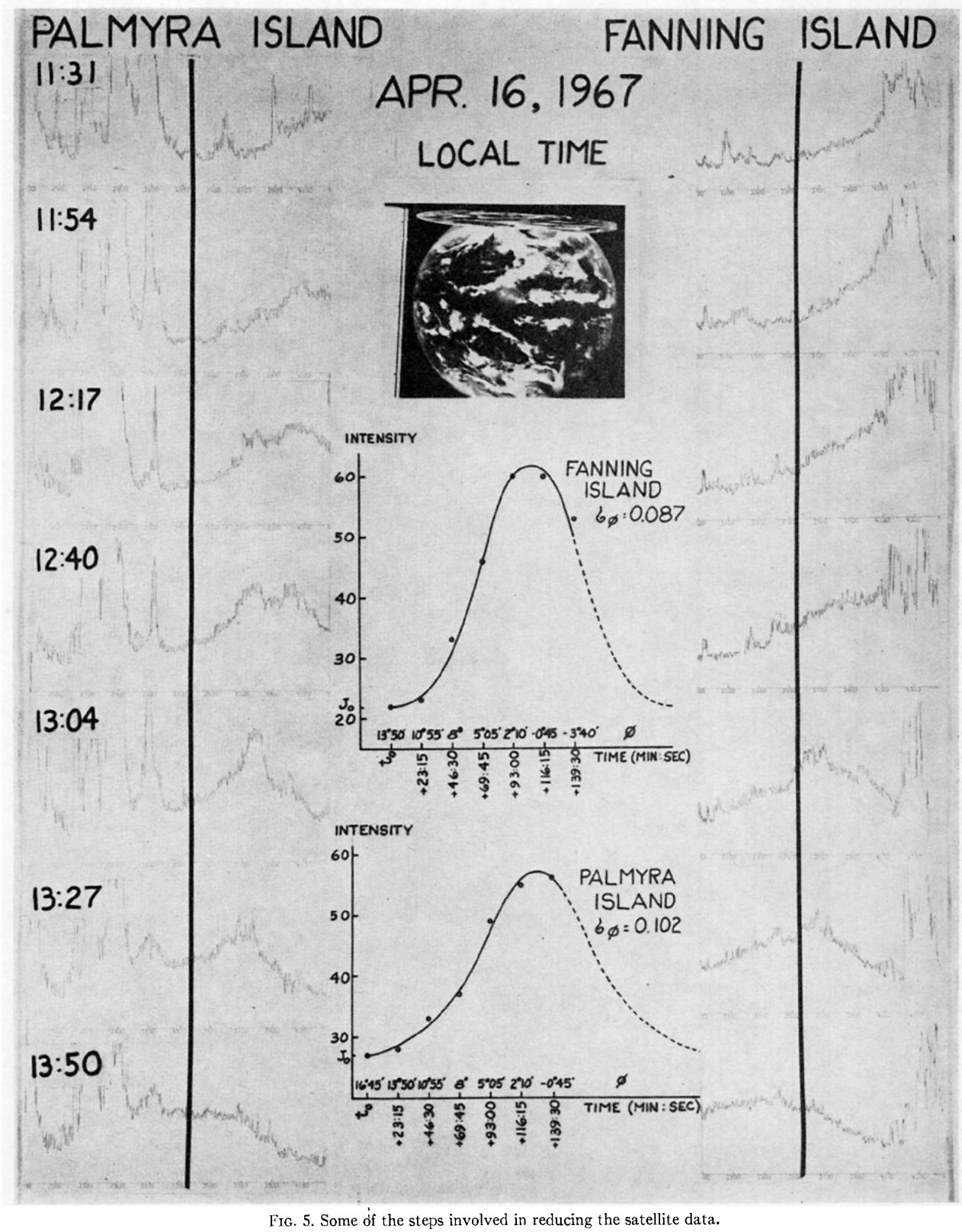

FIG. 5. Some of the steps involved in reducing the satellite data.

8. Results

The comparison between calculated scalar winds and actual wind measurements were made on two dates (16 and 19 April 1967) for each of the three islands (Palmyra, Fanning and Christmas).

The process of calculating the scalar wind involved the following steps:

1) Plotting those scan lines which include the sun glitter, from a sequence of consecutive pictures.
2) Navigating on each picture to find which line and picture element represent each island location. (There were apparent variations in the line number, between consecutive pictures, because of the spacecraft variable pitch.)
3) Plotting the intensity J as a function of time.
4) Converting time to corresponding east-directed tilt ϕ, using (9).
5) Subtracting the background light.
6) Finding β from (11), and applying the corrections $\cos^4\beta$ in (13), to get values of the probability P (up to a constant). (This correction was significant only in cases where the latitude of the reflecting point was far from the latitude of the horizontal specular line of reflection).
7) Finding the standard deviation of the probability curve.
8) Finding the range of possible wind velocities from Fig. 4.

In Fig. 5 some of these steps are illustrated for two cases, i.e., for Palmyra and Fanning on 16 April 1967. The records on the right side of the figure are eight scan lines over the latitude of Fanning Island, taken in intervals of 23 min, the longitude of the island being marked by the vertical line. These eight intensities yield the normal curve shown in the middle. A similar procedure is shown also for Palmyra Island.

The calculated standard deviation results are plotted against actual wind measurements, as points, in Fig. 4. The numbers in brackets near those points indicate the measured wind direction relative to the east-west direction.

Except for one of the C points which is only 5° from the east-west direction and therefore should have been closer to the σ_u^2 line, all other points are within the limits suggested by Cox and Munk.

9. Conclusions

Our work shows the feasibility of studying the east-west component of the wave slope distribution from a synchronous satellite by using the sun as the radiation source with its movement, relative to the earth, as a scanning mechanism.

Using Cox and Munk's linear relation between the variance of the slope and the wind velocity, it was possible to estimate scalar wind velocities in the area of the sun glitter, and to compare them to actual wind velocity measurements taken on the ocean. These comparisons revealed that the enormous height of the observer did not degrade the accuracy of the observation. When the wind direction is given, the accuracy of the calculated wind velocity is as good as if the sun glitter is studied from aircraft altitude, i.e., ± 1 m sec^{-1}.

Despite the good agreement with ground measurements, some possible sources of error should be pointed out. The method allows for atmospheric backscattered light at the point of interest, by examining the intensity of backscattering when the point is not within the sun glitter pattern. It then assumes that the atmospheric backscattered light remains constant during the measurement period. This may lead to systematic errors if there is a diurnal fluctuation of unresolved clouds and haze. The method avoids clouds by searching for a clear area of at least the size of the telescope resolution in the neighborhood of the point of interest. Clouds of a size below this resolution will interfere with the measurement since their contribution will be too small to prevent making measurement at that point, yet large enough to cause erroneous reading. Avoiding clouds will become easier, the higher the telescope resolution. Another source of error, although rather rare, would be large slicks. If the point of interest is within such a slick, an underestimate of the wind velocity will result.

In the course of this work, it became more and more evident that the sun glitter is a strong and reliable source of radiation that should be studied instead of being avoided. In addition to the geometry of the sea and surface wind velocity, much can be learned about the atmosphere above the sea, since this radiation has crossed the whole atmosphere twice, and the trip is recorded in its spectrum.

Acknowledgments. The author wishes to thank Prof. Verner E. Suomi for many stimulating discussions. Thanks are also due to Mr. Eric Smith for his efforts in the computer programming.

This research was supported by the National Aeronautics and Space Administration under Contract NASw-65.

REFERENCES

Cox, C., and W. Munk, 1954a: Statistics of the sea surface derived from sun glitter. *J. Marine Res.*, **13**, 198–227.

——, and ——, 1954b: Measurement of the roughness of the sea surface from photographs of the sun's glitter. *J. Opt. Soc. Amer.*, **44**, 838–850.

Rozenberg, G. V., and Yu. A. R. Mullamaa, 1965: Some possibilities of determining wind speed over an ocean surface using observations from artificial earth satellites. *Izv. Atmos. Oceanic Phys.*, **1**, 282–290.

Sekera, Z., and W. Viezee, 1961: Distribution of the intensity and polarization of the diffusely reflected light over a planetary disk. Rept. R-389-PR, RAND Corporation, Santa Monica, Calif.

Zipser, E. J., and R. C. Taylor, 1968: A catalogue of meteorological data obtained during the Line Islands Experiment February–April 1967. Rept. TN-35, National Center for Atmospheric Research, Boulder, Colo.